Few-photon electron-positron pair creation in the collision of a relativistic nucleus and an intense x-ray laser beam

C. Müller,[1] A. B. Voitkiv,[2] and N. Grün[1]
[1]*Institute for Theoretical Physics, University of Giessen, Heinrich-Buff-Ring 16, D-35392 Giessen, Germany*
[2]*Max-Planck-Institut für Kernphysik, Saupfercheckweg 1, D-69117 Heidelberg, Germany*
(Received 20 April 2004; published 25 August 2004)

We study the nonlinear process of e^-e^+ pair creation by a nucleus which moves at a relativistic energy in the laboratory frame and collides with an intense x-ray laser beam. The collision system under consideration is chosen in such a way that the simultaneous absorption of at least two photons from the laser wave is required in order to exceed the energy threshold of the reaction. We calculate total and differential rates for both free-free and bound-free pair production. In the case of free-free pair creation we demonstrate the effect of the laser polarization on the spectra of the produced particles, and we show that at very high intensities the total rate exhibits features analogous to those well known from above-threshold ionization rates for atoms. In the case of bound-free pair creation a singularity is found in the laboratory frame angular distribution of the produced positron. This singularity represents a distinct characteristic of the bound-free pair production and allows one to separate this process from free-free pair creation even without detecting a bound state of the captured electron. For both types of pair creation we consider the dependences of the total rates on the collision parameters, give the corresponding scaling laws, and discuss the possibility to observe these nonlinear processes in a future experiment.

DOI: 10.1103/PhysRevA.70.023412 PACS number(s): 42.50.Hz, 25.75.Dw, 32.80.−t

I. INTRODUCTION

The large progress in laser technology over the last two decades has given rise to extensive research activities in the field of laser-matter interactions. The emphasis has mainly been put on the strong-field processes of multiphoton and tunneling ionization or excitation of atoms, molecules, or clusters by intense laser pulses, thereby restricting the focus on systems that are governed by nonrelativistic dynamics (see, e.g., [1,2] and references therein). For the process of strong-field photoionization of atoms also relativistic effects have been studied in some detail (see, e.g., Refs. [3–11]). However, if an atomic system is submitted to a radiation field of extremely high frequency and/or intensity, then not only excitation or ionization can occur but also the reaction channels of e^-e^+ pair creation open. The different processes are schematically depicted in Fig. 1. Within the Dirac sea picture, the process of pair creation can be viewed as the transition of an electron from the negative-energy continuum into a positive-energy state. In the case of free-free pair creation (a) the latter is also a continuum state, while it is a discrete bound state in the case of bound-free pair creation (b). In Fig. 1 also the process of ionization (c) is shown, which is the transition from a positive-energy bound state to the positive-energy continuum. Notice the especially close relation between the processes (b) and (c).

The subject of laser-induced pair production is mainly discussed in connection with the new x-ray free-electron laser (XFEL) facilities [12], presently under construction at SLAC and DESY [13]. They are proposed to yield beams of spatially coherent synchrotron radiation with single-photon energies up to $\omega \sim 10$ keV at intensities close to $I \sim 10^{20}$ W/cm^2, corresponding to an intensity parameter $\xi \sim \sqrt{I}/\omega c$ of the order of 10^{-3} [14]. If an atom, an ion, or a bare nucleus at rest is exposed to such an XFEL field, then, in principle, pair creation is possible but it requires the absorption of $n \sim 100$ laser photons. Therefore, the resulting production rate will be negligibly small, since, as a general rule, the rate for an n-photon process scales as ξ^{2n} in the $\xi \ll 1$ regime.

To overcome this problem, one can make use of a nucleus that is not at rest but moves at a relativistic energy through the laser wave; that is, one can consider pair creation in a laser-nucleus collision [15,16]. Then, in the rest frame of the nucleus, the photon energy is Doppler shifted, which considerably lowers the required number of laser photons to be absorbed. In the case of a head-on collision, the enhancement factor is maximum and given by $(1+\beta)\gamma$ where β is the reduced velocity of the nucleus in the laboratory frame and

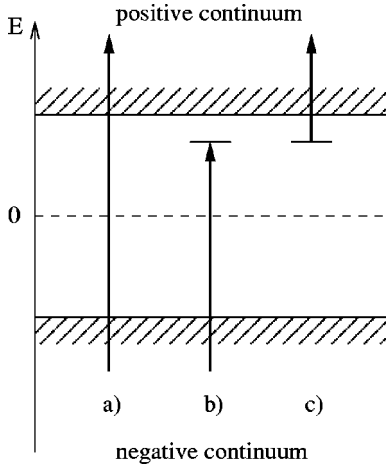

FIG. 1. Schematic sketch of the processes of (a) free-free pair creation, (b) bound-free pair creation, and (c) ionization.

$\gamma=(1-\beta^2)^{-1/2}$ is its Lorentz factor. Note that the laser electric field strength is equally enhanced in the nucleus frame. In Ref. [15] we focused on the situation where an extremely relativistic nucleus, whose energy lies in the range of the upcoming large hadron collider at CERN, is moving through a superintense near-optical laser wave. Under those circumstances the pair creation can be viewed as a quasistatic tunneling process.

In contrast to this high-intensity and low-frequency (i.e., $\xi \gg 1$) scenario, we consider in the present paper the complementary low-intensity and high-frequency (i.e., $\xi \ll 1$) situation—that is, pair production in the collision of a moderately relativistic nucleus and an XFEL beam. The parameters of the colliding system are chosen such that the absorption of at least two photons is required in order to surmount the energy threshold of the reaction. Pair creation by two-photon absorption is the lowest order of multiphoton or nonlinear pair production. Note that the corresponding linear process—i.e., pair creation by a single γ quantum of sufficiently high energy in the Coulomb field of a nucleus—was considered long ago [17]. We study both free-free and bound-free nonlinear pair production where, in the latter case, the created electron is simultanuously captured into a bound state of the projectile nucleus. We calculate the total reaction rates as well as the energetic and angular distributions of one of the produced leptons. While in Refs. [15,16] we treated a circularly polarized laser field only, in the present paper we also consider the numerically more involved case of a linearly polarized wave and demonstrate the influence of the laser polarization on the particle spectra. Notice that the effect of the laser polarization on the total production rate in the $\xi \gg 1$ regime (i.e., the tunneling regime) has been discussed in Ref. [18]. Furthermore, we extend the presentation of two-photon bound-free pair creation given in our Letter [16], where this nonlinear process was considered for the first time.

Before we start our consideration, a last remark may be in order. A few years ago, the nonlinear process of free-free e^-e^+ pair creation in the collision of an ultrarelativistic *electron* beam with an intense optical laser pulse was experimentally observed at SLAC [19]. This process seems to be closely related to the free-free pair production in highly energetic nucleus-laser collisions. However, the very important difference between these two processes is that, according to the theoretical analysis in Ref. [19], the pair production in the electron-laser collision mainly proceeds via an indirect mechanism where first a high-energy photon is produced by Compton backscattering, which afterwards creates a pair by interacting with the optical photons. Since the Compton cross section strongly depends on the mass of the scattering particle, the two-step process is suppressed by several orders of magnitude in the case of a *heavy* projectile like a nucleus (cf. also the discussion in Ref. [15]). Therefore, in the present paper the two-step mechanism for pair production is not taken into account.

II. THEORY

A. General

When we consider pair creation in a laser-nucleus collision, we have to treat the lepton motion in the combined electromagnetic fields of the nucleus and laser wave. That is, we have to deal with the Hamiltonian [20]

$$H = -\mathrm{i}c\boldsymbol{\alpha}\cdot\boldsymbol{\nabla} + \gamma^0 c^2 - A_N^0 + \boldsymbol{\alpha}\cdot\boldsymbol{A}_L, \tag{1}$$

which, for simplicity, is taken in the rest frame of the nucleus. Here, $A_N^0=Z/|\boldsymbol{x}|$ is the nuclear Coulomb potential and $A_L^\mu=(0,\boldsymbol{A}_L)$ denotes the laser four-potential taken in the radiation gauge. In general, the transition amplitude for a quantum mechanical process can be expressed in two equivalent ways, either in the post form (see, e.g., [21])

$$(S-1)_{fi} = -\frac{\mathrm{i}}{c}\int [(H-\mathrm{i}\partial_t)\Phi_f]^\dagger \Psi_i d^4x \tag{2}$$

or in the prior form

$$(S-1)_{fi} = \frac{\mathrm{i}}{c}\int \Psi_f^\dagger (H-\mathrm{i}\partial_t)\Phi_i d^4x, \tag{3}$$

where Ψ_i (Ψ_f) is an eigenstate of the full Hamiltonian H, while Φ_f (Φ_i) is an exact asymptotic final (initial) state lacking only the potential that causes the transition. If we chose the latter potential to be the nuclear Coulomb potential, then the prior form amplitude for pair creation can be written as

$$(S-1)_{fi} = -\frac{\mathrm{i}}{c}\int \Psi_f^\dagger A_N^0 \psi_{p,s}^{(+)} d^4x, \tag{4}$$

with the negative continuum Volkov state $\psi_{p,s}^{(+)}$ describing the outgoing positron (see below). For the fully interacting state Ψ_f that describes the motion of the produced electron, no analytical expression is known. In the following subsections we will therefore employ physically reasonable approximations to Ψ_f that are suited for the treatment of free-free and bound-free pair production, respectively.

Beforehand, we note that in this paper the laser field is described by a classical, monochromatic plane wave with the wave vector $k^\mu=\omega/c(1,\mathbf{e}_z)$ and the amplitude a, which is either linearly polarized,

$$A_L^\mu(x) = a_1^\mu \cos\,\eta, \tag{5}$$

or circularly polarized,

$$A_L^\mu(x) = a_1^\mu \cos\,\eta + a_2^\mu \sin\,\eta. \tag{6}$$

Here, $\eta=(kx)$, $a_1^\mu=a(0,\mathbf{e}_x)$, and $a_2^\mu=a(0,\mathbf{e}_y)$. The Dirac equation $(\mathrm{i}\partial\!\!\!/+A\!\!\!/_L/c-c)\Psi=0$ in such a transversal plane wave is exactly solved by the Volkov states [22,23]

$$\psi_{p,s}^{(\pm)}(x) = N_p\left(1 \pm \frac{k\!\!\!/A\!\!\!/_L}{2c(kp)}\right)u_{p,s}^{(\pm)}\mathrm{e}^{\mathrm{i}f^{(\pm)}(x)}, \tag{7}$$

with

$$f^{(\pm)}(x) = \pm(px) + \frac{1}{c(kp)}\int^\eta \left[(pA_L) \mp \frac{1}{2c}A_L^2\right]d\eta'.$$

The indices $(\pm)$ refer to the charge of the corresponding Dirac particle, p^μ and s are its (free) four-momentum and spin projection, respectively, and $u_{p,s}^{(\pm)}$ denotes a free Dirac spinor [24]. The normalization constant is conveniently cho-

sen as $N_p=\sqrt{c/q^0}$, where $q^0=E_q/c$ is the zeroth component of the so-called effective four-momentum,

$$q^\mu = p^\mu + \frac{\overline{\boldsymbol{A}_L^2}}{2c^2(kp)}k^\mu \tag{8}$$

which characterizes the motion of an otherwise free Dirac particle in a laser wave; here $\overline{\boldsymbol{A}_L^2}=\xi^2c^4$ denotes the time-averaged square of the laser amplitude, where the dimensionless quantity ξ is the intensity parameter. By the Lorentz scalar $q^2=m_*^2c^2$, the effective mass m_* of the leptons in the laser field is defined. Note that, due to the small value of ξ, the effective momentum and the asymptotic free momentum practically coincide in the high-frequency field of an XFEL.

B. Free-free pair creation

First, we consider the case of free-free pair creation where not only the positron but also the electron is produced in a continuum state [cf. Fig. 1(a)]. If the electron velocity v_- with respect to the nucleus is not too small (i.e., if $Z/v_- \ll 1$), then the influence of the laser field should be dominant in comparison with the nuclear Coulomb field. For this reason, one may describe the outgoing e^- state by a corresponding positive continuum Volkov state and find in this way from Eq. (4) the approximate amplitude

$$(S-1)_{\rm ff} = -\frac{\mathrm{i}}{c}\int [\psi^{(-)}_{p_-,s_-}]^\dagger A_N^0 \psi^{(+)}_{p_+,s_+} d^4x \tag{9}$$

for free-free (ff) pair creation. Clearly, up to an overall sign, we would have found the same expression, if we had started from the post-form amplitude (2) instead. The integral in Eq. (9) can be solved analytically by Fourier expansion with the use of the generating function of the Bessel functions J_n [25]. The resulting fully differential production rate can be expressed in the form

$$d^6R_{\rm ff} = \frac{cZ^2}{2\pi^3}\sum_{n\geqslant n_0}\sum_{s_\pm}|M^{(n)}_{p_-p_+}|^2\frac{\delta(Q_n^0)}{Q_n^4}\frac{d^3q_+}{q_+^0}\frac{d^3q_-}{q_-^0}, \tag{10}$$

where the first sum runs over the number of absorbed laser photons, beginning with the smallest possible number n_0, $Q_n^\mu=q_+^\mu+q_-^\mu-nk^\mu$ is the four-momentum transfer to the nucleus, and the $M^{(n)}_{p_-p_+}$ denote some reduced amplitudes.

In the case of a circularly polarized laser wave of the form (6) these reduced amplitudes read [15]

$$M^{(n)}_{p_-p_+} = \overline{u}^{(-)}_{p_-,s_-}\left\{\left(\not\epsilon - \frac{a^2(\epsilon k)}{2c^2(kp_+)(kp_-)}\not k\right)B_n + \left(\frac{\not\epsilon\not k\not a_1}{2c(kp_+)} - \frac{\not a_1\not k\not\epsilon}{2c(kp_-)}\right)C_n + \left(\frac{\not\epsilon\not k\not a_2}{2c(kp_+)} - \frac{\not a_2\not k\not\epsilon}{2c(kp_-)}\right)D_n\right\}u^{(+)}_{p_+,s_+}, \tag{11}$$

with $\epsilon=(1,\mathbf{0})$ such that $\not\epsilon=\gamma^0$ and the coefficients

$$B_n = J_n(\overline{\alpha})\mathrm{e}^{\mathrm{i}n\eta_0},$$

$$C_n = \frac{1}{2}[J_{n+1}(\overline{\alpha})\mathrm{e}^{\mathrm{i}(n+1)\eta_0} + J_{n-1}(\overline{\alpha})\mathrm{e}^{\mathrm{i}(n-1)\eta_0}],$$

$$D_n = \frac{1}{2i}[J_{n+1}(\overline{\alpha})\mathrm{e}^{\mathrm{i}(n+1)\eta_0} - J_{n-1}(\overline{\alpha})\mathrm{e}^{\mathrm{i}(n-1)\eta_0}]. \tag{12}$$

Here, we have used the abbreviations $\overline{\alpha}=(\alpha_1^2+\alpha_2^2)^{1/2}$ and $\eta_0=\arccos(\alpha_1/\overline{\alpha})=\arcsin(\alpha_2/\overline{\alpha})$ with

$$\alpha_j = \frac{(a_jp_-)}{c(kp_-)} - \frac{(a_jp_+)}{c(kp_+)} \tag{13}$$

for $j=1,2$.

In the case of a linearly polarized laser wave of the form (5) we have instead

$$M^{(n)}_{p_-p_+} = \overline{u}^{(-)}_{p_-,s_-}\left\{\not\epsilon B_n + \left[\frac{\not\epsilon\not k\not a_0}{2c(kp_+)} - \frac{\not a_0\not k\not\epsilon}{2c(kp_-)}\right]C_n - \frac{a^2(\epsilon k)\not k}{2c^2(kp_+)(kp_-)}D_n\right\}u^{(+)}_{p_+,s_+}. \tag{14}$$

This time, the so-called generalized Bessel functions $\tilde{J}_n$ (see, e.g., [26]) enter the coefficients:

$$B_n = \tilde{J}_n(\alpha_1,\alpha_2),$$

$$C_n = \frac{1}{2}[\tilde{J}_{n-1}(\alpha_1,\alpha_2) + \tilde{J}_{n+1}(\alpha_1,\alpha_2)],$$

$$D_n = \frac{1}{4}[\tilde{J}_{n-2}(\alpha_1,\alpha_2) + 2\tilde{J}_n(\alpha_1,\alpha_2) + \tilde{J}_{n+2}(\alpha_1,\alpha_2)]. \tag{15}$$

Here,

$$\tilde{J}_n(\alpha_1,\alpha_2) = \sum_{m=-\infty}^{\infty} J_{n-2m}(\alpha_1)J_m(\alpha_2), \tag{16}$$

with

$$\alpha_1 = \left[\frac{(a_1p_-)}{c(kp_-)} - \frac{(a_1p_+)}{c(kp_+)}\right], \quad \alpha_2 = -\frac{a^2}{8c^2}\left[\frac{1}{(kp_-)} + \frac{1}{(kp_+)}\right]. \tag{17}$$

C. Bound-free pair creation

In the case of pair production with capture the electron is created in a bound state of the nucleus [cf. Fig. 1(b)]. Speaking of a bound Coulomb state in the presence of a laser wave implies that this state still keeps its main properties as a bound state and, therefore, a clear physical meaning can be attributed to this state. This is guaranteed, e.g., if the nuclear field strength F_N experienced by the bound electron is significantly larger than the peak laser field strength F_L (taken in the nuclear rest frame). In such a case, the effect of the laser wave on the bound electron should be less important than that of the nuclear Coulomb field. Under such circumstances, in Eq. (4) one may use the approximation $\Psi_f\approx\phi_{1s}$, where ϕ_{1s} is the Coulomb ground state. We chose the ground state to represent the bound system because most of the electrons are expected to be captured into the K shell since it can accomodate larger momenta. We thus arrive at the approximate amplitude

$$(S-1)_{\rm bf} = -\frac{\rm i}{c}\int \phi_{1s}^{\dagger} A_N^0 \psi_{p,s_+}^{(+)} d^4x \tag{18}$$

for bound-free (bf) pair creation. If, instead, we had started from the post form version (2) and had employed a corresponding approximation to Ψ_i, then we would have got the slightly different expression

$$(\tilde{S}-1)_{\rm bf} = \frac{\rm i}{c}\int \phi_{1s}^{\dagger}\boldsymbol{\alpha}\cdot\boldsymbol{A}_L\psi_{p,s_+}^{(+)} d^4x = -\frac{\rm i}{c}\int \overline{\phi}_{1s}\mathcal{A}_L\psi_{p,s_+}^{(+)} d^4x. \tag{19}$$

One can, however, show that both forms yield identical transition rates since the amplitudes (18) and (19) differ by a (total) time derivative only. Note, moreover, that the approximations that Eqs. (18) and (19) are based upon are essentially similar to those used in the so-called strong-field approximation theories [26–28] which are widely applied in the theoretical treatment of laser-atom interactions.

We now want to derive in some detail the differential pair creation rate, since this was omitted in Ref. [16]. The derivation is more conveniently performed starting from the post-form amplitude (19). Further, in contrast to our treatment of free-free pair production, we restrict ourselves to the case of a circularly polarized laser beam [cf. Eq. (6)]. We perform the calculation in the rest frame of the nucleus: i.e., in what follows all quantities are to be taken in this frame. Note that this derivation is similar to that given in Ref. [3] where the strong-field photoionization of a hydrogenlike ion was considered.

The ground-state wave function in Eq. (19) can be written as

$$\phi_{1s}(x) = g(r)\chi_{s_-}(\vartheta,\varphi)\mathrm{e}^{-\mathrm{i}E_{1s}t},$$

where the radial wave function $g(r)$ and the spinors $\chi_{s_-}(\vartheta,\varphi)$ are taken from Ref. [24]. The fully differential production rate is essentially given by the square of the amplitude (19) summed over the particle spins:

$$\begin{aligned}\mathcal{J} &= \sum_{s_\pm}|(\tilde{S}-1)_{\rm bf}|^2 \\ &= \frac{1}{cq^0}\sum_{s_\pm}\int d^4x\int d^4x'\,\mathrm{e}^{-\mathrm{i}[f^{(+)}(x)-f^{(+)}(x')+E_{1s}(t-t')]}g(r)g(r') \\ &\quad\times\overline{u}_{p,s_+}^{(+)}\left(1+\frac{\mathcal{A}_L\not{k}}{2c(kp)}\right)\mathcal{A}_L\chi_{s_-}\overline{\chi'}_{s_-}\mathcal{A}_L'\left(1+\frac{\not{k}\mathcal{A}_L'}{2c(kp)}\right)u_{p,s_+}^{(+)}.\end{aligned} \tag{20}$$

Here, $E_{1s}=\sigma c^2$ with $\sigma=[1-(\alpha Z)^2]^{1/2}$ is the ground-state energy, and functions that depend on x' rather than on x are marked by a prime—e.g., $A_L'=A_L(x')$. The electron-spin sum in Eq. (20) can be carried out explicitly by calculating the matrix

$$M = \sum_{s_-}\chi_{s_-}\overline{\chi'}_{s_-}. \tag{21}$$

Then, the positron spin sum can be evaluated in the usual way as

$$\mathcal{T} = \sum_{s_+}\overline{u}_{p,s_+}^{(+)}\Gamma u_{p,s_+}^{(+)} = \frac{1}{2c}\mathrm{Tr}\{\Gamma(\not{p}-c)\}, \tag{22}$$

with

$$\Gamma = \left(\mathcal{A}_L+\frac{a^2}{2c(kp)}\not{k}\right)M\left(\mathcal{A}_L'+\frac{a^2}{2c(kp)}\not{k}\right).$$

Hence, we get

$$\mathcal{J} = \frac{1}{cq^0}\int d^4x\int d^4x'\,\mathrm{e}^{-i[f^{(+)}(x)-f^{(+)}(x')+E_{1s}(t-t')]}g(r)g(r')\mathcal{T}. \tag{23}$$

This integral can be solved analytically by expanding the exponential into a Fourier series. The result for the doubly differential transition rate (per unit time) is

$$\frac{d^2R_{\rm bf}}{dE_q d\cos\theta_q} = 4\frac{a^2}{Z^3}\sum_{n\geqslant n_0}|\boldsymbol{q}|\frac{(u_A+u_B+u_C)}{[1+(\rho/Z)^2]^4}\delta(E_q+E_{1s}-n\omega), \tag{24}$$

with the smallest possible number of photons n_0, $\rho=|\boldsymbol{q}-n\boldsymbol{k}|$, and

$$\begin{aligned}u_A &= \frac{\mathcal{P}}{c}\{([J_{n-1}(\zeta)]^2+[J_{n+1}(\zeta)]^2)[(p_0+c)\sigma^2(\rho/Z)^4\mathcal{U}^2+(p_0 \\ &\quad -c)\tau^2(\rho/Z)^2\mathcal{V}^2-(2/Z)p_z\sigma\tau(\rho/Z)^2(p_z-bk_z)\mathcal{U}\mathcal{V}] \\ &\quad +(4/Z)J_{n-1}(\zeta)J_{n+1}(\zeta)\sigma\tau(\rho/Z)^2p_\perp^2\mathcal{U}\mathcal{V}\},\end{aligned}$$

$$\begin{aligned}u_B &= -2\frac{\omega}{c^2}(\rho/Z)^2\mathcal{P}n[J_n(\zeta)]^2[\sigma^2(\rho/Z)^2\mathcal{U}^2+\tau^2\mathcal{V}^2+(2/Z)\sigma\tau(p_0 \\ &\quad +bk_z-2p_z)\mathcal{U}\mathcal{V}],\end{aligned}$$

$$\begin{aligned}u_C &= \frac{a^2}{c^3(p_0-p_z)}\mathcal{P}[J_n(\zeta)]^2(\rho/Z)^2[\sigma^2(\rho/Z)^2\mathcal{U}^2+\tau^2\mathcal{V}^2 \\ &\quad -(2/Z)\sigma\tau(p_z-bk_z)\mathcal{U}\mathcal{V}].\end{aligned} \tag{25}$$

Furthermore, in Eq. (25) we have used the abbreviations $\tau=(1-\sigma)/\alpha Z$, $p_\perp=|\boldsymbol{p}|\sin\theta_p$, $\zeta=ap_\perp/c(kp)$, $b=n-a^2/2c^2(kp)$, and

$$\mathcal{P} = \frac{(1+\sigma)[\Gamma(\sigma)]^2 2^{2(\sigma-1)}}{\Gamma(1+2\sigma)}\frac{[1+(\rho/Z)^2]^{2-\sigma}}{(\rho/Z)^6},$$

$$\mathcal{U} = \sin\mathcal{X}+(\rho/Z)\cos\mathcal{X},$$

$$\mathcal{V} = \sigma(\rho/Z)\cos\mathcal{X}-[1+(1+\sigma)(\rho/Z)^2]\sin\mathcal{X},$$

$$\mathcal{X} = \sigma\arctan(\rho/Z). \tag{26}$$

III. RESULTS AND DISCUSSION

A. Free-free pair creation

In this subsection we present our results on free-free pair production by a proton colliding at $\gamma=50$ head-on with an

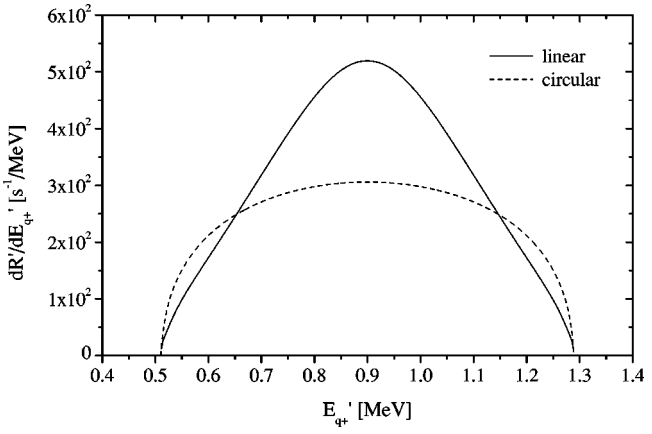

FIG. 2. Projectile frame rates, differential in the positron energy E'_{q+}, for free-free pair creation by a proton colliding at $\gamma=50$ with an intense XFEL ($\omega=9$ keV, $I=8\times10^{19}$ W/cm^2) of linear or circular polarization.

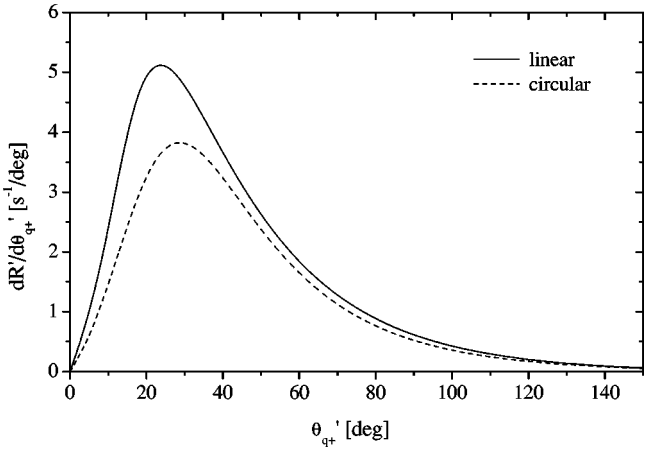

FIG. 3. Projectile frame rates for free-free pair creation, differential in the polar emission angle θ'_{q+} of the positron. The parameters of the colliding system are the same as in Fig. 2.

intense x-ray laser of 9 keV photon energy that is either linearly or circularly polarized. We mainly focus on the situation where the laser wave has an intensity of 8×10^{19} W/cm^2 (i.e., $\xi=7.5\times10^{-4}$). This corresponds to a constant electric field strength of $F_L=1.8\times10^{11}$ V/cm in the case of a circularly polarized wave and to a peak field strength of $F_L=2.5\times10^{11}$ V/cm in the case of a linearly polarized wave. In the rest frame of the nucleus, the laser frequency and field strength are enhanced by the factor $(1+\beta)\gamma\approx100$. Hence, the energetic threshold for pair creation can be surmounted by the absorption of at least two photons from the laser wave. As long as $\xi\ll1$, the relative contribution of the higher photon orders ($n\geqslant3$) is proportional to ξ^2 and, thus, negligible. Clearly, this argument does not hold any longer if the value of ξ approaches unity. Therefore, at the end of the subsection we want to slightly broaden its scope by discussing some results on few-photon pair creation in the $\xi\approx1$ transition regime.

In the following, we use primed quantities in the nuclear rest frame and unprimed quantities in the laboratory frame.

1. Positron spectra: Polarization effects

First we discuss the energetic and angular distributions of the produced particles. Within our approach, which is of first order in the nuclear Coulomb potential, the spectra for the emitted electron and the emitted positron are identical. For definiteness, all figures refer to the produced positron. We give the differential rates with respect to the effective positron momentum q_+^μ, which is practically identical with the observable free momentum p_+^μ [cf. Eq. (8) and the following remark]. In principle, the spectra shown are thus directly accessible to an experiment.

We start with the positron spectra in the rest frame of the proton. As Fig. 2 shows, the energy spectra in this frame are symmetric about the mean value of 900 keV, where they attain a maximum. This maximum is more pronounced in the case of a linearly polarized laser beam. Clearly, the symmetry arises from the fact that in the approximation used the distributions are identical for both leptons. Figure 3 shows the production rates differential in the positron emission angle with respect to the laser beam direction. The angular distributions for linear and circular laser polarization are very similar. In both cases the particles are mainly emitted under angles of about $\sim30°$. While the polar angle distributions of Fig. 3 for linear and circular laser polarization are very similar in shape, the azimuthal angle spectra, shown in Fig. 4, display a very distinct polarization effect. In the case of a linearly polarized wave about 40% more positrons are emitted along the polarization axis than perpendicular to it [cf. Eq. (5)], whereas in the case of a circularly polarized wave the distribution is isotropic due to obvious symmetry reasons. In addition, we note that the electron and positron are preferably emitted with (almost) opposite transversal momenta—i.e., with a large relative transversal velocity. For this reason, the final-state Coulomb interaction between the electron and positron is small, which justifies its neglect in our treatment.

We now turn to the corresponding positron spectra in the laboratory frame. Note that the laboratory frame and the nucleus frame are connected by a Lorentz boost along the

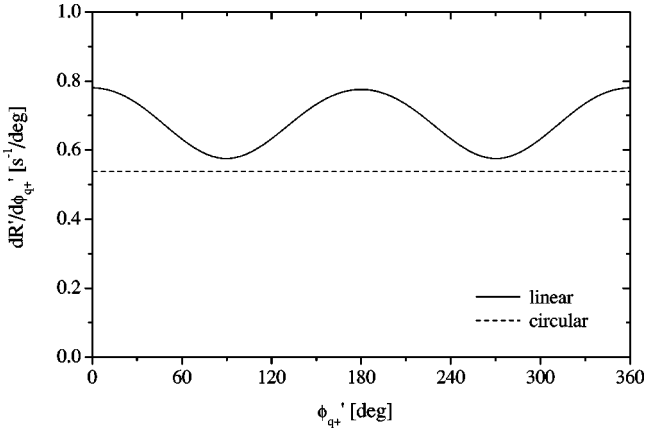

FIG. 4. Projectile frame rates for free pair creation, differential in the azimuthal emission angle ϕ'_{q+} of the positron. The parameters of the colliding system are the same as in Fig. 2.

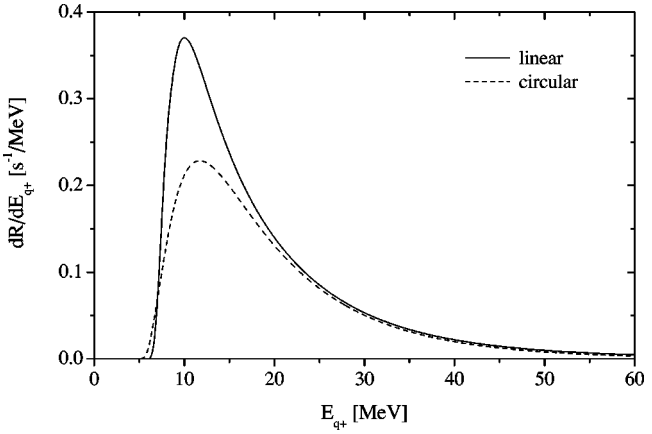

FIG. 5. Laboratory-frame rates for free-free pair creation, differential in the laboratory-frame energy E_{q+} of the positron. The parameters of the colliding system are the same as in Fig. 2.

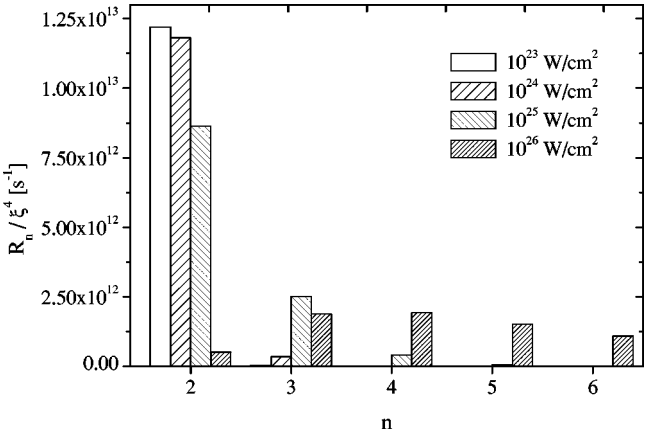

FIG. 7. Partial laboratory-frame rates for free-free pair creation by a proton colliding at $\gamma=50$ with a circularly polarized XFEL of 9 keV photon energy for different values of the laboratory-frame laser intensity.

beam axis. Figure 5 shows the laboratory-frame energy spectra. The main contribution to the total rate comes from positrons in the energy range 8 MeV$\lesssim E_{q+}\lesssim$30 MeV. For energies below $\sim$20 MeV the differential rate is considerably larger for a linearly polarized wave, whereas for higher energies the results for both polarizations practically coincide. Figure 6 shows the laboratory-frame rate differential in the polar emission angle θ_{q+} of the positron with respect to the propagation direction of the laser beam. The particles are emitted within a narrow cone around the backward direction—that is, under small angles of typically 1.5° with respect to the proton beam direction. This is similar to our results on free-free pair creation in the tunneling regime [15]. We note that the azimuthal angle spectrum in the laboratory frame differs from the nuclear frame spectrum shown in Fig. 4 only by an overall constant factor of γ^{-1}, which is due to time dilation.

2. Total rates: Above threshold pair creation

Integration of the differential rates yields a total laboratory-frame production rate of 4.8 s^{-1} for linear polarization and of 3.8 s^{-1} for circular polarization; this means that on average $\sim 2\times10^{-13}$ pairs are produced per collision if we assume the laser beam to have a finite duration of 100 fs. Further we note that also in the tunneling regime a linearly polarized laser wave is more efficient for pair creation than a wave of circular polarization [18]. A similar polarization effect is also known from the perturbative treatment of strong-field photoionization [29].

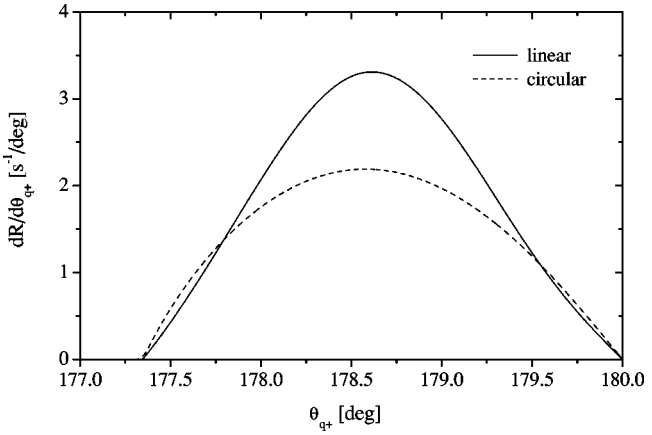

FIG. 6. Laboratory-frame rates for free-free pair creation, differential in the polar emission angle θ_{q+} of the positron. The parameters of the colliding system are the same as in Fig. 2.

In agreement with the general scaling law mentioned in the Introduction, the nonlinear production rates are proportional to ξ^4 or I^2, respectively, unless the laser intensity amounts to or exceeds $\sim 10^{25}$ W/cm^2, which corresponds to a value of the intensity parameter close to unity. For such high intensities the contributions from the higher photon orders ($n\geqslant 3$) become non-negligible, as Fig. 7 shows, where the partial rates for pair creation by absorption of two to six photons are given. For $I=10^{25}$ W/cm^2 the contributions from the higher photon orders are already considerable, while for $I=10^{26}$ W/cm^2 they even exceed the contribution from $n=2$. An analogous phenomenon is known from the above-threshold ionization (ATI) of atoms in strong laser fields (see, e.g., [1]). Similarly as for the ATI, the above threshold pair creation at $\xi\gtrsim 1$ forms a bridge between the multiphoton pair creation ($\xi<1$) studied in this paper and the tunneling pair creation ($\xi\gg 1$) considered in Ref. [15].

B. Bound-free pair creation

In this subsection we consider bound-free pair creation by a heavy nucleus that collides at a Lorentz factor of $\gamma=50$ head-on with an intense x-ray laser ($\omega=9$ keV, $\xi=7.5\times10^{-4}$) of circular polarization. The corresponding laser field strength and intensity amount to $F_L=1.8\times10^{11}$ V/cm and $I=8\times10^{19}$ W/cm^2. The nuclear charge is chosen as $Z=50$ such that the K-shell Coulomb field of $F_N\approx Z^3\times5.14\times10^9$ V/cm is about 40 times larger than the laser electric field strength of $F_L'\approx 1.8\times10^{13}$ V/cm in the nuclear rest frame. The binding energy of a K-shell electron amounts to $E_K=E_{1s}-c^2=35$ keV. The photon energy in the nucleus

frame is $\omega' \approx 900$ keV. Here and in the following we use primed quantities in the rest frame of the nucleus and unprimed quantities in the laboratory frame. Hence, as before, the threshold for pair creation can be exceeded by the absorption of at least two photons, whereas the contribution of the higher photon orders (i.e., $n \geqslant 3$) is negligibly small.

Furthermore, we note the following facts: The ponderomotive energy $E_{\mathrm{pond}} = \xi^2 c^2/2 \approx 0.15$ eV of a free electron in such a laser wave is orders of magnitude smaller than the K-shell binding energy E_K. Similarly, the radius $r_{\mathrm{osc}} = \xi c/\omega' \sim 10^{-14}$ cm and the velocity $v_{\mathrm{osc}} = \xi c \sim 10^7$ cm/s of the laser-induced quiver motion are many times smaller than the K-shell radius $r_K \approx 10^{-10}$ cm and the K-shell orbital velocity $v_K \approx \alpha Z c \approx 10^{10}$ cm/s. Moreover, a rough estimate shows [30] the lifetime of the bound hydrogenlike system in the laser wave to be orders of magnitude longer than the K-shell orbiting time $2\pi r_K/v_K \approx 10^{-19}$ s. All this gives further evidence that the Coulomb state of the bound electron in the presence of the laser field has a direct physical meaning. On the other hand, neglecting the higher photon orders and the small ponderomotive effects, the created positron is emitted with a fixed kinetic energy of about 800 keV in the nucleus frame. This corresponds to a positron velocity of $v_+ \approx 126$ a.u. and, hence, to a rather small ratio of $Z/v_+ \approx 0.4$. The Volkov description of the outgoing positron can therefore be regarded a reasonable approximation.

1. Positron spectra

First we present our results on the angular and energetic distributions of the produced positron. For comparison, we have also calculated the corresponding rates for linear bound-free pair creation by the absorption of a single photon of twice the energy from an equally intense laser wave. Also for comparison, we further give the differential rates for two-photon free-free pair creation by simply scaling our results on free-free pair production by proton impact by the factor Z^2 (cf. Sec. III A). For the positrons originating from nonlinear bound-free pair creation we will use the shorthand notation "bound-free positrons." Accordingly, the "one-photon positrons" and "free-free positrons" are those produced by linear bound-free pair creation and nonlinear free-free pair creation, respectively.

Figure 8 shows the angular spectra of the created positrons in the nuclear rest frame. The emission angle is measured with respect to the propagation direction of the laser beam. The angular distribution attains a maximum at $\sim 10° - 15°$ in the cases of nonlinear and linear bound-free pair creation and at $\sim 30°$ in the case of nonlinear free-free pair creation. Since the emission angle is, roughly speaking, inversely proportional to the emission momentum, the different positions of these maxima are due to the fact that the kinetic energy of the free-free positrons is, on average, half as large as the fixed kinetic energy of the bound-free and the one-photon positrons (cf. Fig. 2). For the same reason, the comparatively broad energetic distribution of the free-free positrons gives rise to an angular distribution that is broader than the distributions of the other positrons. Comparing the quite similar spectra of the bound-free and one-photon positrons, we notice that the distribution of the latter is slightly

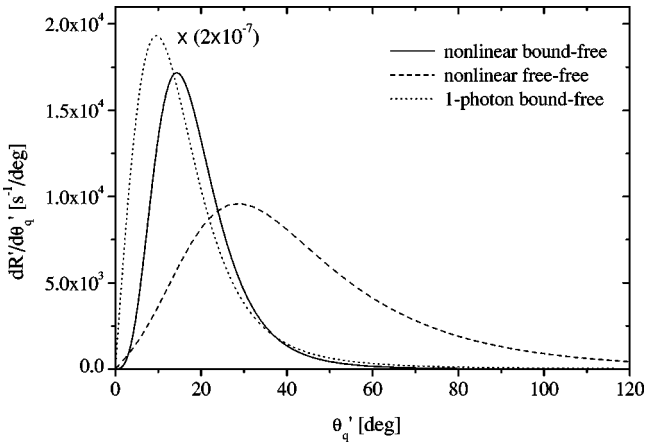

FIG. 8. Projectile frame rates, differential in the polar emission angle θ_q' of the positron, for nonlinear free-free and bound-free pair creation in the collision of a relativistic heavy nucleus ($Z=50$, $\gamma=50$) and an intense XFEL ($\omega=9$ keV, $I=8\times10^{19}$ W/cm^2). Also shown is the rate for bound-free pair creation by a single photon of 18 keV.

shifted to smaller emission angles. From a theoretical point of view this shift is due to the small argument behavior of the Bessel function $J_0(\zeta)$ that, according to Eq. (25), appears in the one-photon rate but not in the nonlinear rate. The absolute values of the one-photon rate are orders of magnitude larger because of the weaker intensity dependence.

Now we turn to the differential production rates in the laboratory frame. As Fig. 9 shows, here the energies of the bound-free and one-photon positrons roughly amount to 6 MeV $\lesssim E_q \lesssim$ 12 MeV, which is noticeably smaller than the typical energies of the free-free positrons. Note that small emission angles in the nucleus frame correspond to small emission energies in the laboratory frame. The one-photon spectrum exhibits an interesting feature since, unlike the nonlinear spectra, it is a monotonously decreasing function with the maximum value at the smallest possible positron energy. This qualitative distinction is caused by the above-

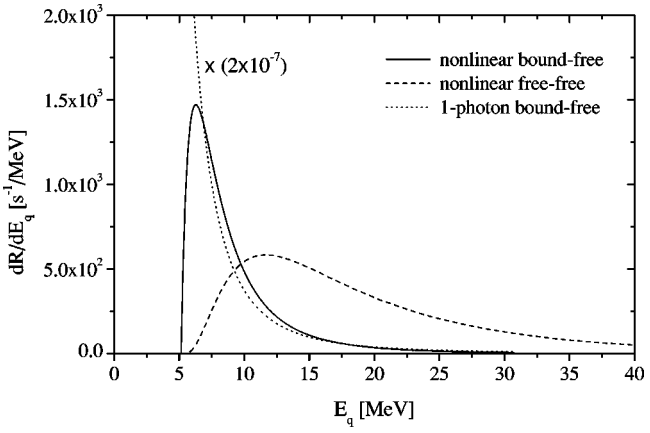

FIG. 9. Laboratory-frame rates for free-free and bound-free pair creation, differential in the energy E_q of the positron. The parameters of the colliding system are the same as in Fig. 8. Also shown is the rate for bound-free pair creation by a single photon of 18 keV.

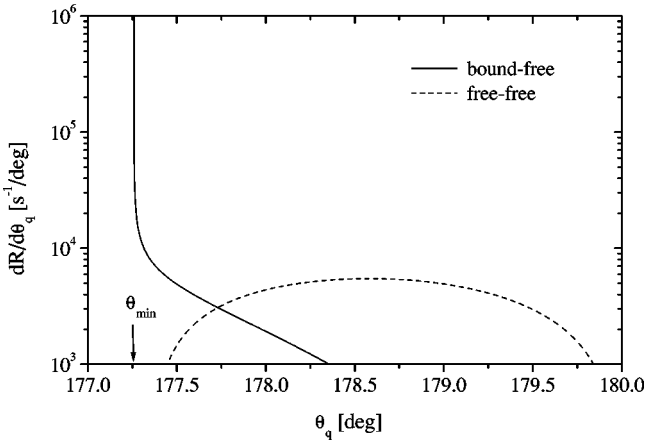

FIG. 10. Laboratory-frame rates for nonlinear free-free and bound-free pair creation, differential in the polar emission angle θ_q of the positron. The parameters of the colliding system are the same as in Fig. 8.

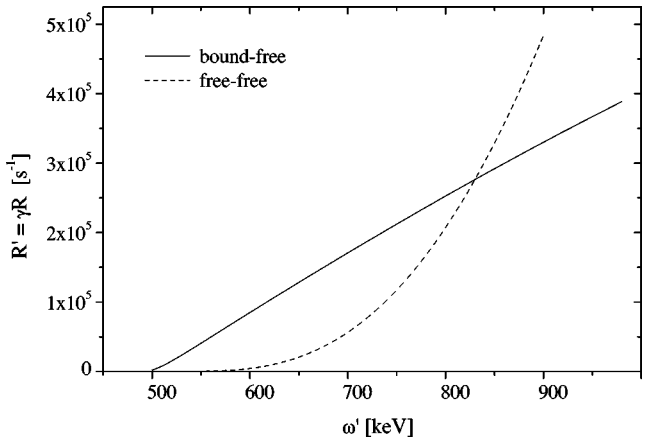

FIG. 11. Total nuclear-frame rates for two-photon pair creation as a function of the nuclear frame photon energy for $Z=50$, $\gamma=50$, and $\xi=7.5\times10^{-4}$.

mentioned slightly different behavior of the nucleus-frame angular distribution of the one-photon positrons at small angles (cf. Fig. 8).

Figure 10 shows the angular distributions of the bound-free and free-free positrons in the laboratory frame. In sharp contrast to the corresponding angular spectra in the nucleus frame (cf. Fig. 8) the laboratory frame distributions are highly different from one another. While the free-free positrons smoothly cover the narrow angular range between, say, 177.5° and 179.8°, practically all bound-free positrons are emitted into the angle 177.25°, thereby forming an almost discrete spectrum located slightly below the continuous free-free spectrum. This singularity arises from the fact that the fixed positron velocity v_+ in the nucleus frame is smaller than the relative velocity between the two frames of reference (cf. Refs. [16,21]). One can show that the angle, where the singularity appears, coincides with the smallest possible emission angle that, for kinematical reasons, is accessible to the positrons. This minimum angle $\theta_{\min}$ is given by

$$\sin\theta_{\min}=\frac{\gamma_+\beta_+}{\gamma\beta}, \tag{27}$$

with $\beta_+=v_+/c$ and $\gamma_+=(1-\beta_+^2)^{-1/2}$. The same argument holds for the one-photon positrons; i.e., their angular spectrum exhibits the same singularity (and is therefore not shown in Fig. 10). To the free-free positrons, however, this argument does not apply since their energy in the nuclear rest frame is not fixed but varies over a broad range. Thus, in some sense one may say that the fixed emission energy of the bound-free positrons in the nucleus frame leads to a (practically) fixed emission angle in the laboratory frame.

2. Total rates: Scaling behavior

When we integrate the laboratory-frame spectra shown above, we get total rates of $R_{\rm bf}=6.5\times10^3\ {\rm s}^{-1}$ for nonlinear bound-free pair creation and $R_{\rm ff}=9.6\times10^3\ {\rm s}^{-1}$ for nonlinear free-free pair creation. This means, if we assume the projectile nucleus to collide with a finite laser pulse of 100 fs length, then we can give the rough estimate that, on average, 3.3×10^{-10} bound-free and 4.8×10^{-10} free-free pairs are created per collision. The corresponding rate for the one-photon process (with the double-photon energy) is much larger and amounts to $4.0\times10^{10}\ {\rm s}^{-1}$.

From our numerical calculations we can also determine the dependences of the total rates for two-photon pair production on the collision parameters Z, γ, ξ, and ω. Clearly, both rates scale as ξ^4 in the $\xi\ll1$ regime. Further, $R_{\rm bf}\propto Z^5$ shows the typical Z dependence of a capture process [21] whereas, according to Eq. (10), $R_{\rm ff}$ scales as Z^2. Note that the total rates in the nucleus frame, $R'=\gamma R$, can depend on the remaining parameters γ and ω only through the combination $\omega'=(1+\beta)\gamma\omega\approx2\gamma\omega$. As Fig. 11 shows, $R'_{\rm bf}$ is proportional to ω' while $R'_{\rm ff}$ increases with its third power. Thus, in summary, the scaling behavior of the total rates for two-photon pair production is given by

$$R_{\rm bf}\propto\gamma^{-1}Z^5\xi^4(\omega'-\omega_{\min}),$$

$$R_{\rm ff}\propto\gamma^{-1}Z^2\xi^4(\omega'-\omega_{\min})^3, \tag{28}$$

with $\omega_{\min}$ denoting the respective threshold frequencies for two-photon pair creation (i.e., $2\omega_{\min}=m_*c^2+E_{1s}$ in the case of bound-free pair creation and $2\omega_{\min}=2m_*c^2$ in the case of free-free pair creation). We stress, however, that both our theoretical approaches are not justified near to these thresholds since the influence of the nuclear Coulomb field on the resulting low-energy leptons is not small.

IV. SUMMARY AND CONCLUSION

We have considered the strong-field processes of free-free and bound-free e^-e^+ pair creation by few-photon absorption in the collision of a relativistic nucleus and an intense x-ray laser beam. We mainly focused on a situation where the pair production occurs by the simultaneous absorption of two photons while the contribution of the higher photon orders is negligibly small. We discussed in detail the resulting angular and energetic distributions of one of the emitted particles. In

the case of free-free pair creation a particular emphasis was laid on the effect of the laser polarization on the lepton spectra. In the case of bound-free pair creation we found that the positron spectra are mainly governed by kinematical constraints. Further, the scaling behavior of the total production rates was analyzed. In addition to these two-photon creation processes we briefly discussed a situation where, due to an increasing laser intensity, also higher photon orders are contributing. Under such circumstances the production process may be called *above-threshold pair creation* (in analogy with the well-known ATI).

Finally, we briefly address the question whether the nonlinear processes of free-free and bound-free pair creation can be observed in experiment. According to our results, the total production rates are rather small. Nevertheless, since the created leptons are emitted with high energy into a narrow angular cone, they should be accessible to a measurement. We further note that the free-free and bound-free reaction channels can be clearly discriminated from each other, either by taking advantage of the qualitatively different angular distributions of the emitted positrons or by aiming at the (coincident) detection of the created electrons. In the case of bound-free pair creation the latter would mean to detect the hydrogenlike ion formed by the projectile nucleus and the captured electron. A rough estimate shows that the majority of these ions will survive the passage through the laser beam [16,30].

[1] M.H. Mittleman, *Introduction to the Theory of Laser-Atom Interactions* (Plenum Press, New York, 1982).

[2] N.B. Delone and V.P. Krainov, *Multiphoton Processes in Atoms* (Springer, Berlin, 2000).

[3] H.R. Reiss, J. Opt. Soc. Am. B **7**, 574 (1990); Prog. Quantum Electron. **16**, 1 (1992).

[4] Relativistic Effects in Strong Electromagnetic Fields, edited by J.H. Eberly [Opt. Express **2**(7), 261 (1998)].

[5] J. Ortner and V.M. Rylyuk, Phys. Rev. A **61**, 033403 (2000).

[6] N. Milosevic, V.P. Krainov, and T. Brabec, Phys. Rev. Lett. **89**, 193001 (2002).

[7] P. Koval, S. Fritzsche, and A. Surzhykov, J. Phys. B **36**, 873 (2003).

[8] D.B. Milosevic and F. Ehlotzky, Adv. At., Mol., Opt. Phys. **49**, 373 (2003).

[9] A. Staudt, J. Prager, and C.H. Keitel, Europhys. Lett. **62**, 691 (2003).

[10] C.J. Joachain and N.J. Kylstra, Phys. Scr. **68**, C72 (2003).

[11] G. Mocken and C.H. Keitel, Phys. Rev. Lett. **91**, 173202 (2003).

[12] A. Ringwald, Phys. Lett. B **510**, 107 (2001); V.S. Popov, JETP Lett. **74**, 133 (2001); R. Alkofer, M.B. Hecht, C.D. Roberts, S.M. Schmidt, and D.V. Vinnik, Phys. Rev. Lett. **87**, 193902 (2001).

[13] *The X-ray Free Electron Laser*, TESLA Technical Design Report, edited by G. Materlik and T. Tschentscher (DESY, Hamburg, 2001), Vol. V; J. Arthur, Rev. Sci. Instrum. **73**, 1393 (2002).

[14] Note that a plane laser wave alone, independent of its frequency and intensity, cannot extract pairs from the vacuum [cf. J. Schwinger, Phys. Rev. **82**, 664 (1951)].

[15] C. Müller, A.B. Voitkiv, and N. Grün, Phys. Rev. A **67**, 063407 (2003).

[16] C. Müller, A.B. Voitkiv, and N. Grün, Phys. Rev. Lett. **91**, 223601 (2003).

[17] H.A. Bethe and W. Heitler, Proc. R. Soc. London, Ser. A **146**, 83 (1934); E. Fermi and G.E. Uhlenbeck, Phys. Rev. **44**, 510 (1933) [cf. also C.A. Bertulani and G. Baur, Phys. Rep. **163**, 299 (1988)].

[18] M.H. Mittleman, Phys. Rev. A **35**, 4624 (1987).

[19] D. Burke *et al.*, Phys. Rev. Lett. **79**, 1626 (1997); C. Bamber *et al.*, Phys. Rev. D **60**, 092004 (1999).

[20] Throughout this paper we use a.u., except where otherwise stated. Further, we denote the scalar product of two four-vectors $a^\mu=(a^0,\mathbf{a})$ and $b^\mu=(b^0,\mathbf{b})$ by $(ab)=a^0b^0-\mathbf{ab}$, and we employ Feynman slash notation: $\not{a}=(\gamma a)$.

[21] J. Eichler and W.E. Meyerhof, *Relativistic Atomic Collisions* (Academic Press, San Diego, 1995).

[22] D.M. Volkov, Z. Phys. **94**, 250 (1935).

[23] V.B. Berestetskii, E.M. Lifshitz, and L.P. Pitaevskii, *Relativistic Quantum Theory* (Pergamon Press, Oxford, 1971).

[24] J.D. Bjorken and S.D. Drell, *Relativistic Quantum Mechanics* (McGraw-Hill, New York, 1964).

[25] M. Abramowitz and I.A. Stegun, *Handbook of Mathematical Functions* (Dover, New York, 1965).

[26] H.R. Reiss, Phys. Rev. A **22**, 1786 (1980).

[27] L.V. Keldysh, Zh. Eksp. Teor. Fiz. **47**, 1945 (1964) [Sov. Phys. JETP **20**, 1307 (1965)].

[28] F.H. M. Faisal, J. Phys. B **6**, L89 (1973).

[29] K.J. LaGattuta, Phys. Rev. A **43**, 5157 (1991).

[30] The bound system can decay by photoionization or inelastic photon (Compton) scattering. Using standard formulas, we estimate the corresponding decay rates as 10^{13} s^{-1} and 10^{12} s^{-1}, respectively. Thus, the lifetime of the hydrogenlike ion amounts to $\sim 10^{-13}$ s in the nuclear rest frame.